ELECTRONIC SUPPORTING INFORMATION

Production of Ultra-Deep Sulfur-Free Diesels Using Sustainable Catalytic System Based on UiO-66(Zr)

Carlos M. Granadeiro,[*a] Susana O. Ribeiro,[a] Mohamed Karmaoui,[b] Rita Valença,[c] Jorge C. Ribeiro,[c] Baltazar de Castro,[a] Luís Cunha-Silva[a] and Salete S. Balula[*a]

[a]*REQUIMTE & Department of Chemistry and Biochemistry , Faculty of Sciences, University of Porto, 4169-007 Porto, Portugal*

[b]*Department of Materials and Ceramic Engineering, CICECO, University of Aveiro, 3810-193 Aveiro, Portugal*

[c]*Galp Energia, Refinaria de Matosinhos, 4452-852 Leça da Palmeira, Matosinhos, Portugal*

Experimental

General

All the reagents used in the preparation of the composite material, such as zirconium(IV) chloride (Aldrich), benzene-1,4-dicarboxylic acid (Aldrich), *N,N*-dimethylformamide (DMF, Aldrich), trifluoroacetic acid (TFA, Riedel-de Haën) were used as received without further purification. The reagents used in the ODS processes, dibenzothiophene (DBT, Aldrich), 4-methyldibenzothiophene (4-MDBT, Aldrich) and 4,6-dimethyldibenzothiophene (4,6-DMDBT, Alfa Aesar GmbH & Co KG), acetonitrile (MeCN, Panreac), ethyl acetate (Merck) H_2O_2 30% (Aldrich) and *n*-octane (Aldrich) were also used as received. The untreated diesel sample was supplied by Galp Energia containing approximately 2300 ppm of sulfur and without any previous treatment.

Characterization

FT-IR spectra were obtained on a Jasco 460 Plus spectrometer using KBr pellets, while the FT-Raman spectra were acquired on a RFS-100 Bruker FT-spectrometer, equipped with Nd:YAG laser with a 1064 nm excitation wavelength and laser power set to 350 mW. Powder X-ray diffraction patterns were obtained at room temperature on a X'Pert MPD Philips diffractometer, equipped with an X'Celerator detector and a flat-plate sample holder in a Bragg-Brentano para-focusing optics configuration (45kV, 40 mA). Intensity data were collected by the step-counting method (step 0.04°), in continuous mode, in the *ca.* $3 \leq 2\theta \leq 40°$ range. Scanning electron microscopy (SEM) and electron dispersive X-ray spectroscopy (EDS) studies were performed in a high resolution scanning electron

microscope Quanta 400 FEG ESEM microscope equipped with an EDAX Genesis X4M spectrometer working at 15 kV. Samples were coated with a Au/Pd thin film by sputtering using a SPI Module Sputter Coater equipment. GC-MS analysis were performed using a Hewlett Packard 5890 chromatograph equipped with a Mass Selective Detector MSD series II using helium as the carrier gas (35 cms^{-1}); GC-FID was carried out in a Varian CP-3380 chromatograph to monitor the catalytic reactions. The hydrogen was used as the carrier gas (55 cms^{-1}) and fused silica Supelco capillary columns SPB-5 (30m × 0.25mm i.d.; 25 μm film thickness) were used. The sulfur content in real diesel samples was determined by Energy Dispersive X-Ray Fluorescence Spectrometry using an OXFORD LAB-X, LZ 3125 equipment (ASTM D4294 method) and by Ultraviolet Fluorescence method using a Thermo Scientific equipment with TS-UV module (ISO 20846 method).

Synthesis of UiO-66(Zr) samples

Different UiO-66(Zr) samples were prepared using previously reported experimental procedures. UiO-66 sample was prepared, without acid or modulator, using a modified procedure of the method described by Lillerud *et al*.[1] Briefly, zirconium(IV) chloride (6.4 mmol) and 1,4-benzenedicarboxylic acid (6.4 mmol) were dissolved in DMF (180 mL) at room temperature. The mixture was placed in an oven at 120 ºC for 24 h. After cooling to room temperature, the solid was filtered, washed three times with DMF and ethanol each and dried in an oven at 80 ºC overnight. The samples UiO-66_{HCl}, UiO-66_{mod} and UiO-$66_{HCl,mod}$ were prepared following the method described by De Vos and co-workers.[2] The synthetic route involves the use of HCl as a crystallization agent and/or TFA as a modulator. An initial equimolar solution of zirconium(IV) chloride (0.75 mmol) and 1,4-benzenedicarboxylic acid (0.75 mmol) in DMF (7.75 mL) was prepared. The autoclaves were placed in an oven at 120 ºC for 21 h, after which the solids were recovered by centrifugation, washed three times with DMF and methanol, and dried at 80 ºC overnight.

The crystallinity and extent of linker deficiencies in the framework of the UiO-66(Zr) samples were evaluated by FT-Raman, powder XRD and EDS. The UiO-66 sample was fully characterized, before and after catalytic use, by FT-IR and FT-Raman, powder XRD, SEM and EDS analysis in order to assess the chemical robustness and stability of the catalyst in the ODS process.

Oxidative desulfurization processes (ODS)

ODS of model diesel

The oxidative desulfurization studies were performed using a model diesel containing the most representative refractory sulfur-compounds in diesel, namely dibenzothiophene (DBT), 4-methyldibenzothiophene (4-MDBT) and 4,6-dimethyldibenzothiophene (4,6-DMDBT), in *n*-octane (with a concentration of 500 ppm of sulfur from each compound). The different UiO-66(Zr) samples were tested as heterogeneous catalyst in the ODS process. The reactions were carried out under air in a closed borosilicate reaction vessel with a magnetic

stirrer and immersed in a thermostatically controlled liquid paraffin bath at 50 ºC. The ODS reactions were performed in a biphasic system composed by the model fuel and MeCN. In a typical experiment, the catalyst (15 mg) was added to MeCN (0.75 mL) and model fuel (0.75 mL), and the resulting mixture was stirred for 10 min. The catalytic step of the process is initiated by the addition of aqueous hydrogen peroxide 30% (75 µL). The sulfur content was periodically quantified by GC analysis using tetradecane as a standard. The UiO-66(Zr) samples were tested as catalyst in the ODS process. The amount of catalyst used in the ODS process was optimized for the sample exhibiting the best desulfurization performance (UiO-66). Different ODS experiments were performed using a variable amount of UiO-66 (0.6; 3; 6; 9 and 12 µmol). The recycling studies were performed using the optimized amount of UiO-66 (9 µmol). After each cycle, the catalyst was recovered by filtration, washed thoroughly with acetonitrile, dried in a desiccator over silica gel and reused in a new ODS cycle under the same reactional conditions.

ODS of real diesel

The untreated diesel sample was supplied by Galp Energia containing approximately 2300 ppm of sulfur. An initial extraction was performed using MeCN as the extraction solvent. The biphasic system 1:1 diesel/MeCN was stirred for 10 min at 50 ºC. Afterwards, the diesel was removed from the system and a new portion of clean MeCN was added. This initial extraction procedure was repeated for three time. In the next step, the resulting diesel was mixed with a suspension of the heterogeneous catalyst UiO-66 (120 µmol) in MeCN (1:1 for diesel/MeCN) followed by the addition of the oxidant H_2O_2 (2 mL). The mixture was heated at 50 ºC for 8 h under stirring. After this time, the diesel was removed from the mixture and washed with an equal volume of MeCN at 50 ºC for 10 min. The solid catalyst was also recovered and washed thoroughly with ethyl acetate. The previously oxidized real diesel was treated once more in the presence of the recovered UiO-66 catalyst and using a fresh portion of MeCN and H_2O_2 for 8 h at 50 ºC. At the end of this second catalytic cycle, the treated diesel was recovered from the ODS system and finally washed with MeCN at 50 ºC for 10 min. The sulfur content of the treated diesel was determined through X-ray fluorescence analysis by Galp Energia.

Results and discussion

Characterization of UiO-66(Zr) samples

The FT-Raman spectra of the prepared UiO-66(Zr) samples are compared in Figure S1. Although exhibiting a similar profile, some differences can be observed in the Raman spectra. The bands located at *ca.* 1435 and 860 cm^{-1} provide information concerning the degree of homogeneity of the framework and presence of linker deficiencies.[3] In the ideal UiO-66(Zr) structure, two distinct bands associated with the carboxylate-related stretches are observed in the 1445-1420 cm^{-1} range. The use of HCl as crystallization agent seems to have led to better crystallized frameworks since the spectra of UiO-$66_{HCl,mod}$ and UiO-66_{HCl} show two bands (although not completely separated) associated with the carboxylate stretches. In the other spectra, the presence of a single band in this region suggests differences regarding the presence of carboxylate linkers, namely a higher number of linker defects within the framework.[3]

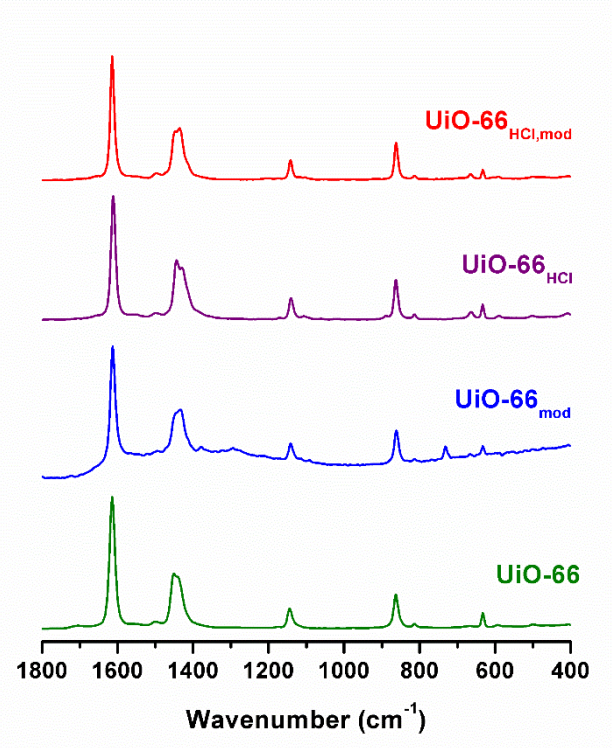

Figure S1. FT-Raman spectra of the UiO-66(Zr) samples prepared by different synthetic procedures.

The XRD patterns of the UiO-66(Zr) samples exhibit the typical diffraction peaks of the MOF in terms of position and relative intensities (Figure S2). It is clear, however that once again the use of HCl during the synthesis results in more crystalline materials.[3,4] In fact, the patterns of UiO-$66_{HCl,mod}$ and UiO-66_{HCl} exhibit sharper and well-resolved peaks, while the patterns of UiO-66 and UiO-66_{mod} display broader peaks suggesting more amorphous materials. In this work, the addition of 10 equivalents of a modulator (TFA) doesn't seem to have significantly influenced the overall crystallization of the materials.

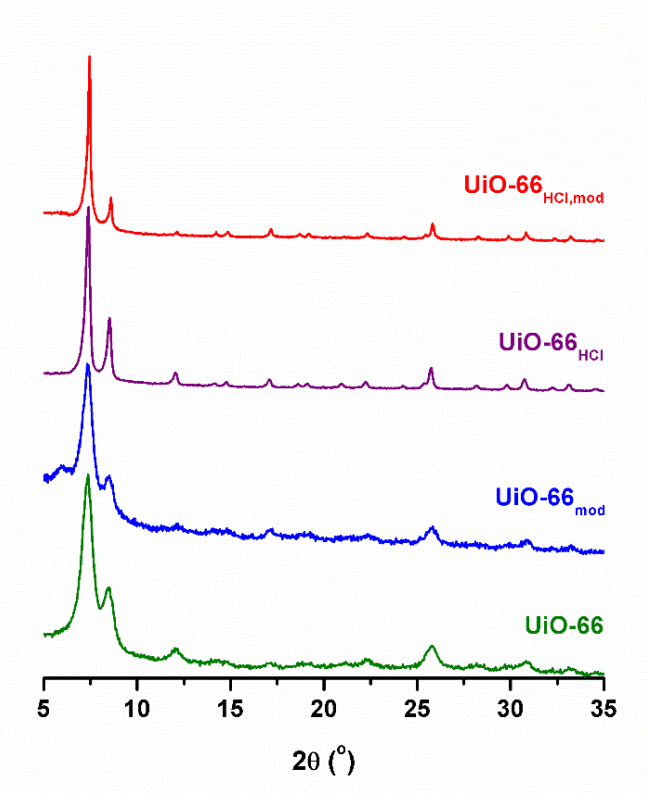

Figure S2. Powder XRD patterns of the UiO-66(Zr) samples.

The chlorine content of the UiO-66(Zr) samples was studied through the quantification of Cl/Zr atomic weight ratios via EDS (Figure S3 and Table S1). The amount of residual chlorine (present even after the material being thoroughly washed) in a UiO-66(Zr) sample provides an indication of the number of defect sites in a material. The random absence of terephthalate ligands throughout the UiO-66(Zr) framework that occurs even in well-crystallized materials, results in charge and coordination deficiencies.[5] Chloride anions can compensate this imbalance by bonding to open zirconium sites, i. e., not coordinated to terephthalate linkers.[2,3]

Regarding the samples prepared through non-modulated synthesis, the UiO-66 exhibits a higher content of chlorine when compared with UiO-66_{HCl}. Considering that the chlorine present in each sample is located in defect sites of the framework, such a result suggests that the extent of linker deficiencies in UiO-66 is higher than in UiO-66_{HCl}. As expected, the samples obtained through modulated synthesis contain a small amount of chlorine according to previously reported data.[2] In fact, De Vos *et al.* have demonstrated that the charge imbalance promoted by the introduction of trifluoroacetate linkers (CF_3COO^-) is compensated by the replacement of OH^- ions by O^{2-} ions in the ideal $[Zr_6(OH)_4O_4]^{12+}$ cluster resulting in a $[Zr_6(OH)_nO_{8-n}]^{(8+n)+}$ (with $n < 4$) cluster.

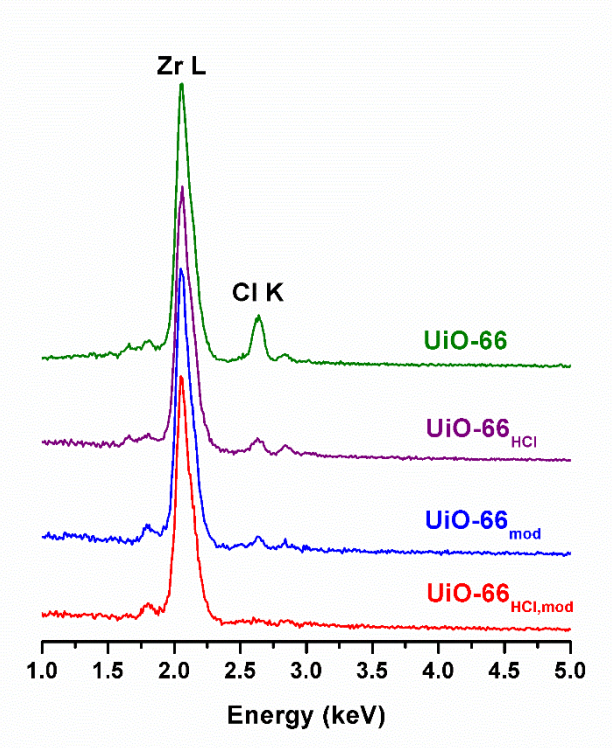

Figure S3. EDS spectra of the UiO-66(Zr) samples in the 1-5 keV range. All spectra are normalized to the Zr L peak.

Table S1. Atomic ratios determined via EDS spectra of the UiO-66(Zr) samples.

Sample	Cl/Zr Atomic ratio
UiO-66	0.34
$UiO\text{-}66_{HCl}$	0.11
$UiO\text{-}66_{mod}$	0.058
$UiO\text{-}66_{HCl,mod}$	0.029

Oxidative desulfurization studies

The UiO-66(Zr) samples were tested as heterogeneous catalysts in the desulfurization of the multicomponent model diesel. The experimental results (Figure S4) show practically complete desulfurization of the multicomponent model diesel after 1 h of reaction using the UiO-66 and UiO-66$_{mod}$ samples. As previously discussed, these samples were prepared without the use of HCl (crystallization agent) resulting in less crystalline samples although still exhibiting the characteristic UiO-66(Zr) framework as shown by the powder XRD patterns (Figure S2). The best desulfurization performance was achieved with the UiO-66 sample with a complete desulfurization of the model diesel after only 30 min of reaction. The well-crystallized UiO-66$_{HCl}$ and UiO-66$_{HCl,mod}$ materials have shown a poorer desulfurization performance. In particular, the UiO-66$_{HCl}$ exhibited no catalytic activity in this ODS system since the desulfurization of the model diesel only occurs during the initial extraction step.

Recent reports correlate the presence of defect sites occurring within several MOF frameworks with the enhancement of the catalytic activity.[6,7] As the ideal and fully coordinated UiO-66(Zr) framework is not expected to exhibit a significant catalytic activity, efforts have been made to promote structural defects while keeping the overall integrity of the framework.[2,5]

In this work, the notable desulfurization performance of the UiO-66 sample is probably related with the low-degree of crystallinity and the considerable number of defect sites in the sample as shown by the amount of residual chlorine via EDS. Comparing the performance of the UiO-66 and UiO-66$_{mod}$ materials (both with a similar degree of crystallinity), one can speculate that the presence of chloride ions at the defect sites, observed in UiO-66, plays a key role in the fast desulfurization observed.

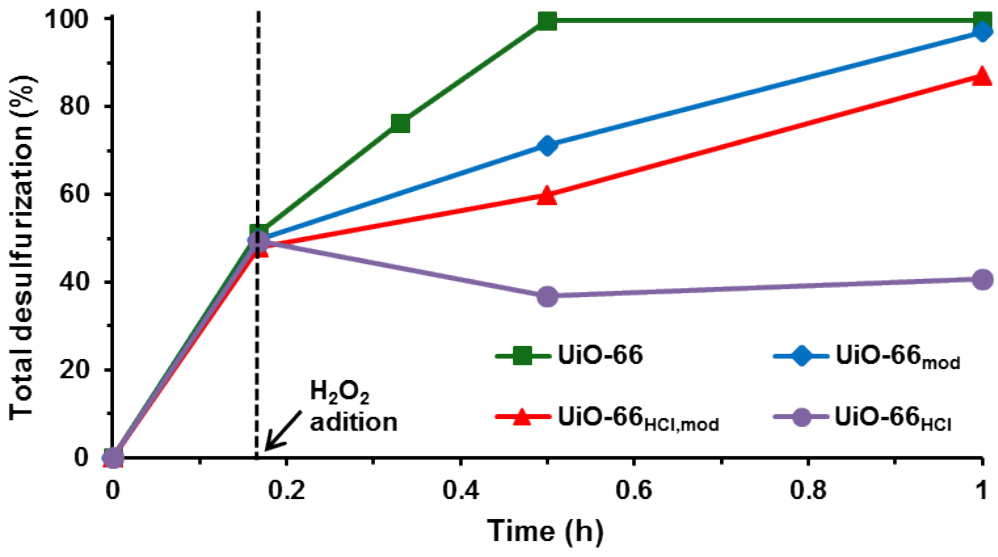

Figure S4. Kinetic profile for the desulfurization process of the model oil using the different UiO-66(Zr) samples showing the initial extraction stage (before the dashed line) and the catalytic step (after the dashed line).

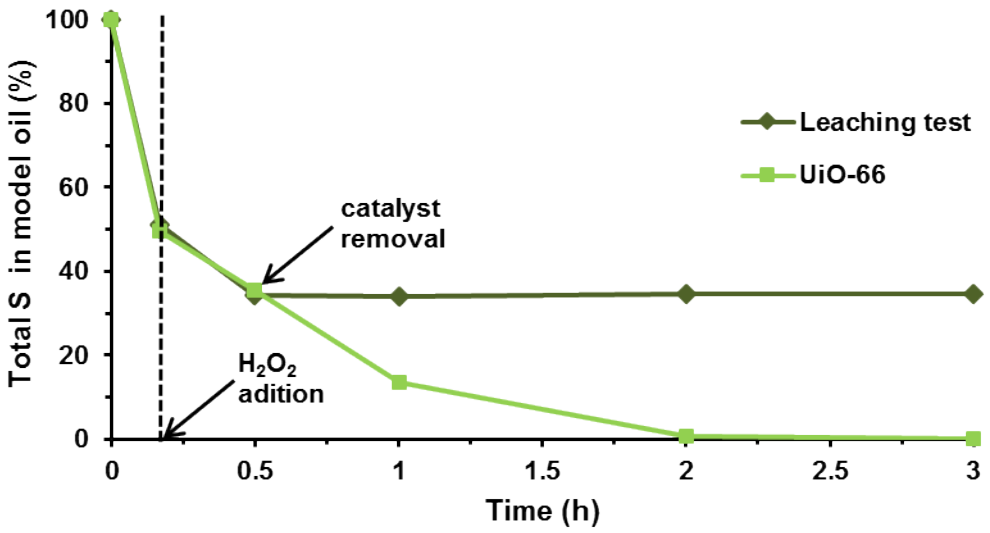

Figure S5. Desulfurization of the multicomponent model diesel using UiO-66 (3 µmol) and the corresponding leaching test (catalyst removal after 30 min of reaction).

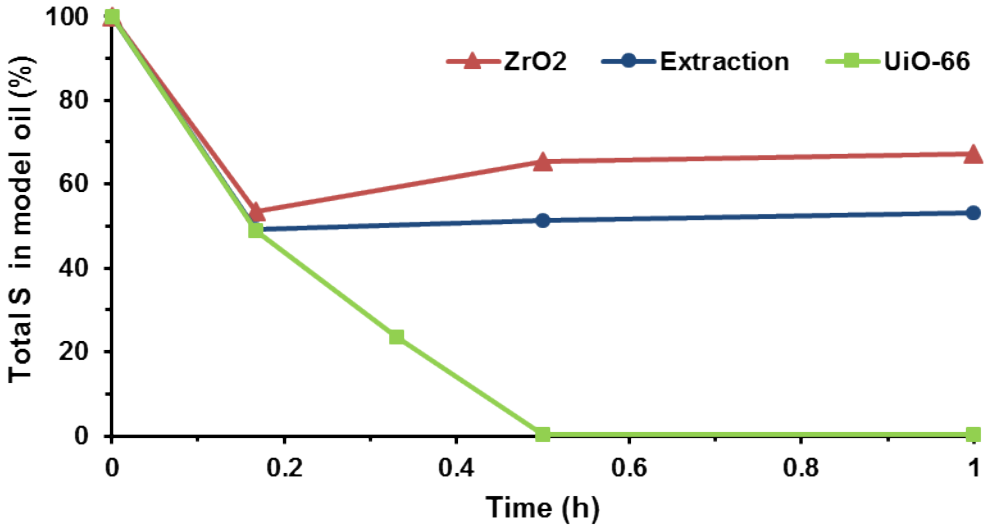

Figure S6. Desulfurization profile of a model diesel in the presence of UiO-66 (9 µmol), performing only the extraction liquid-liquid process, and also combining extraction and catalytic steps in the presence of H_2O_2 oxidant. A control experiment replacing the UiO-66 catalyst by ZrO_2, using an equivalent Zr content (9 µmol), combining extraction and catalytic steps.

Catalyst stability

The structural stability of UiO-66 was evaluated through the extensive characterization of the solid recovered after three consecutive ODS cycles (UiO-66-ac). The vibrational spectroscopy spectra of UiO-66-ac (Figure S7) are very similar to the ones before catalysis. Regarding FT-IR, the typical bands of UiO-66(Zr) remain unaltered,[5] namely the bands assigned to ν_{as}(OCO) and ν_{s}(OCO) stretches located at 1606 and 1373 cm^{-1}, respectively, as well as the ν(Zr-OC) stretches located at 638 and 523 cm^{-1}. The FT-Raman of UiO-66-ac also displays the characteristic UiO-66(Zr) Raman bands[3] including the bands assigned to the intense in-phase aromatic ν(C-C) stretch at 1614 cm^{-1}, the symmetric carboxylate ν_{s}(OCO) at 1433 cm^{-1} and the symmetric C-C ring breathing at 1142 cm^{-1}.

In the powder XRD patterns before and after catalysis, the main diffraction peaks of UiO-66 [2θ = 7.38 (*h*, *k*, *l*, 1, 1, 1), 8.52 (0, 0, 2), 12.03 (0, 2, 2), 17.19 (0, 0, 4), 22.23 (0, 4, 4), 25.77 (0, 0, 6) and 30.82 (1, 1, 7)][8] remain unaffected regarding its position and relative intensity (Figure S8). Both XRD patterns are in good agreement with the data reported in the literature for the UiO-66(Zr) material.[9,10] The SEM images of UiO-66 and UiO-66-ac (Figure S9) show identical morphology for both samples indicating that the morphology of the MOF is not altered during the catalytic ODS cycles. Moreover, the EDS analysis reveals that both samples have an identical chemical composition in terms of elements and their corresponding relative intensity. The combination of evidences from these characterization techniques unequivocally indicates the preservation of the MOF structure without degradation as a result of the remarkable robustness and stability of UiO-66.

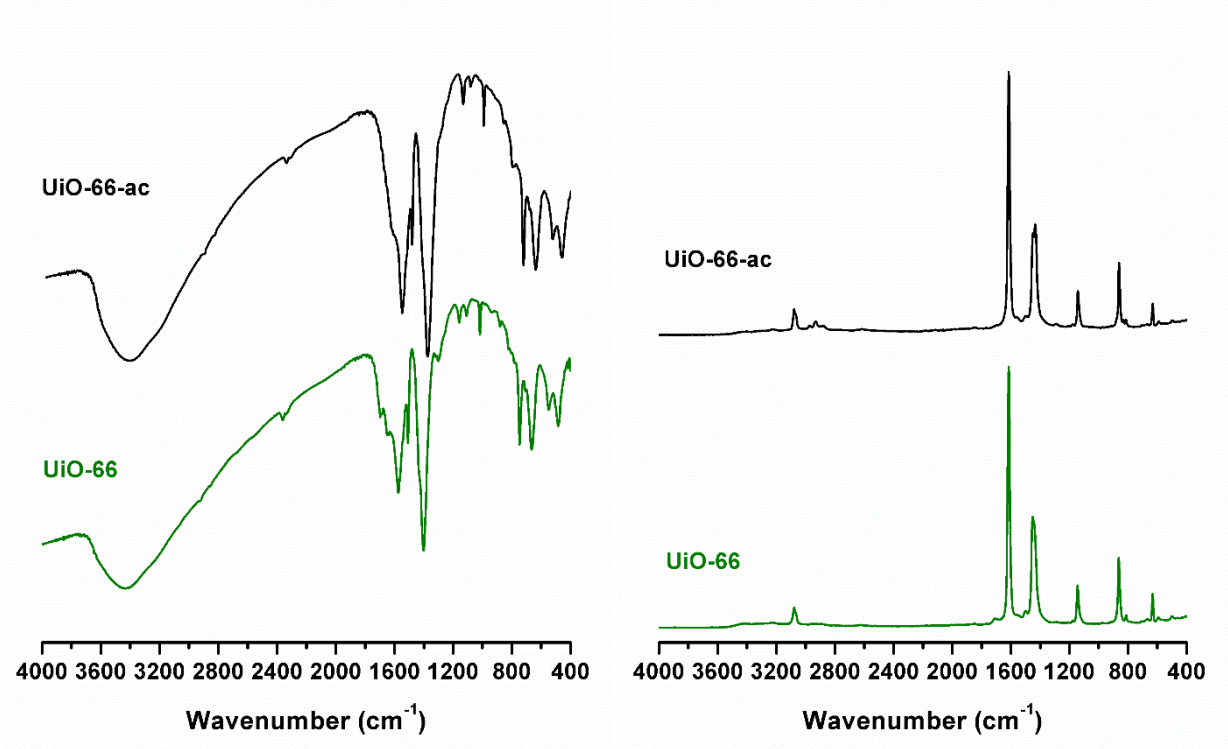

Figure S7. FT-IR (left) and FT-Raman (right) spectra of UiO-66 before and after catalytic use (ac).

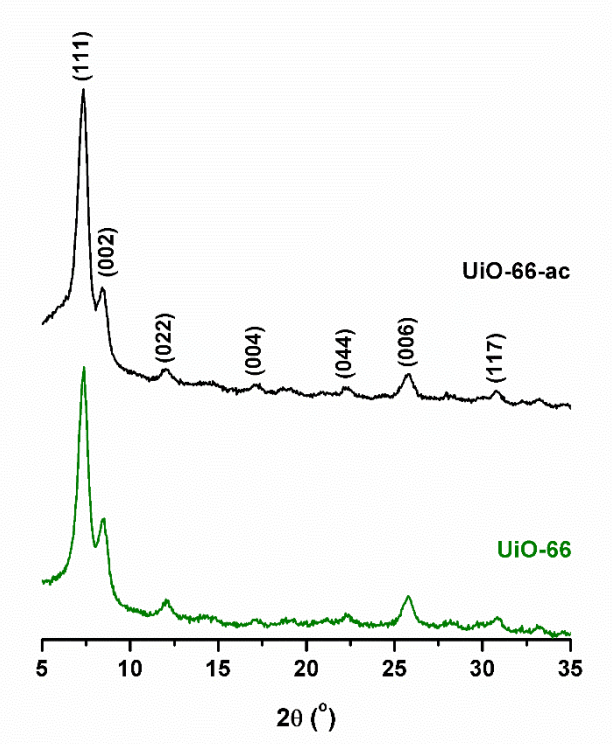

Figure S8. Powder XRD patterns of UiO-66 before and after catalytic use (ac).

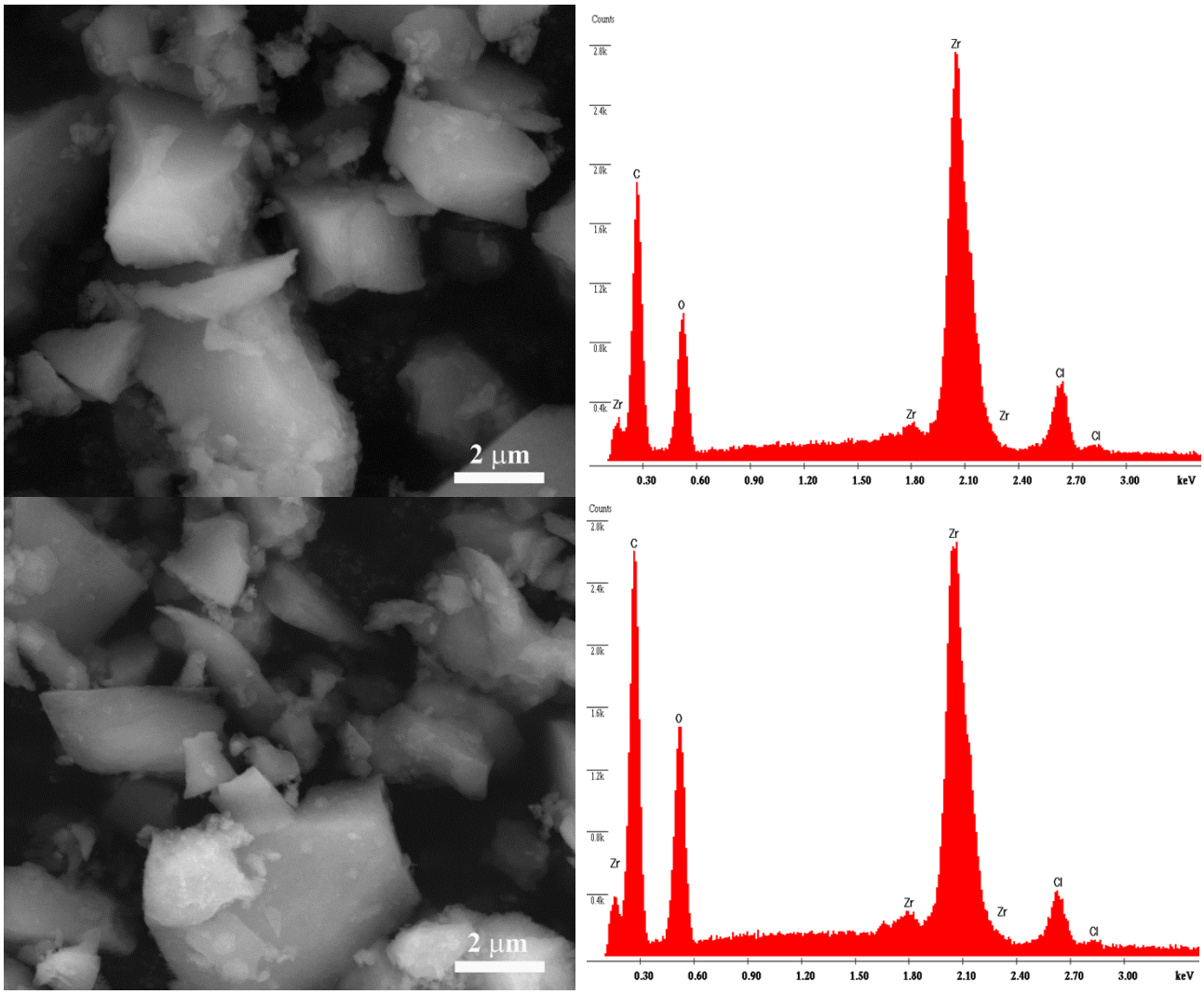

Figure S9. SEM micrographs and EDS spectra of UiO-66 before (left) and after catalysis (right).

References

1. M. Kandiah, M. H. Nilsen, S. Usseglio, S. Jakobsen, U. Olsbye, M. Tilset, C. Larabi, E. A. Quadrelli, F. Bonino and K. P. Lillerud, *Chem. Mater.*, 2010, **22**, 6632–6640.

2. F. Vermoortele, B. Bueken, G. Le Bars, B. V. Voorde, M. Vandichel, K. Houthoofd, A. Vimont, M. Daturi, M. Waroquier, V. Van Speybroeck, C. Kirschhock and D. E. De Vos, *J. Am. Chem. Soc.*, 2013, **135**, 11465-11468.

3. G. C. Shearer, S. Chavan, J. Ethiraj, J. G. Vitillo, S. Svelle, U. Olsbye, C. Lamberti, S. Bordiga and K. P. Lillerud, *Chem. Mater.*, 2014, **26**, 4068-4071.

4. M. J. Katz, Z. J. Brown, Y. J. Colón, P. W. Siu, K. A. Scheidt, R. Q. Snurr, J. T. Hupp and O. K. Farha, *Chem. Commun.*, 2013, 49, 9449-9451.

5. L. Valenzano, B. Civalleri, S. Chavan, S. Bordiga, M. H. Nilsen, S. Jakobsen, K. P. Lillerud and C. Lamberti, *Chem. Mater.*, 2011, **23**, 1700-1718.

6. H. Furukawa, U. Müller and O. M. Yaghi, *Angew. Chem. Int. Ed.*, 2015, **54**, 3417-3430.

7. S. Marx, W. Kleist and A. Baiker, *J. Catal.*, 2011, **281**, 76-87.

8. R. Wu, X. Qian, K. Zhou, H. Liu, B. Yadian, J. Wei, H. Zhu and Y. Huang, *J. Mater. Chem. A*, 2013, **1**, 14294-14299.

9. J. H. Cavka, S. Jakobsen, U. Olsbye, N. Guillou, C. Lamberti, S. Bordiga and K. P. Lillerud, *J. Am. Chem. Soc.*, 2008, **130**, 13850-13851.

10. F. Vermoortele, R. Ameloot, A. Vimont, C. Serre and D. De Vos, *Chem. Commun.*, 2011, **47**, 1521-1523.